SYNTHESIS, SELECTIVE LASER SINTERING AND INFILTRATION OF HIGH T_c DUAL PHASE Ag-YBa$_2$Cu$_3$O$_{7-x}$ SUPERCONDUCTOR COMPOSITES.

Mukesh K. Agarwala, David L. Bourell, Arumugam Manthiram,
Britton R. Birmingham, and Harris L. Marcus.
Center For Materials Science and Engineering.
The University of Texas at Austin, Austin, Texas 78712.

ABSTRACT

Fine, homogeneous dual phase Ag-YBa$_2$Cu$_3$O$_{7-x}$ composite powders were prepared by a simple colloidal sol-gel co-precipitation technique. Silver did not react with or degrade YBa$_2$Cu$_3$O$_{7-x}$. Bulk porous samples of pure YBa$_2$Cu$_3$O$_{7-x}$ and Ag-YBa$_2$Cu$_3$O$_{7-x}$ were made from powders by Selective Laser Sintering. The porous parts were further densified by infiltrating silver into pores, resulting in a dense, structurally sound dual phase superconducting composite. Laser processing parameters were varied to obtain optimum microstructure. The laser sintered parts required oxygen annealing after infiltration to restore the orthorhombic, superconducting structure. X-ray diffraction and T_c measurements indicate some impurity phases present in samples processed under aggressive laser conditions.

INTRODUCTION

Since the discovery of high T_c ceramic superconductors (1) much work has been devoted to develop them for practical applications. Considerable success has been achieved in the area of thin films (2). However, prototype applications in bulk form are still being investigated. The major obstacles in making practical bulk shapes from these materials are their inferior current carrying capacity in bulk form and poor mechanical properties. Numerous synthesis and fabrication techniques have been attempted to tackle these issues, but with limited success.

In the synthesis of these materials, several elements and compounds have been incorporated in the YBa$_2$Cu$_3$O$_{7-x}$ ceramic superconductor either as substitutional elements in the YBa$_2$Cu$_3$O$_{7-x}$ structure or as dispersoids in the YBa$_2$Cu$_3$O$_{7-x}$ matrix (3,4). Noble metals, gold and silver, are one such class of additives that have been widely investigated and found to be promising (3-6). Due to its inertness, silver does not react with and degrade the superconducting properties of the ceramic YBa$_2$Cu$_3$O$_{7-x}$ and has, therefore, been used as an appropriate second phase and as a sheath or cladding material in bulk fabrication (3,6). Silver doping has been found to improve the critical current density, due to the presence of silver at voids between the YBa$_2$Cu$_3$O$_7$ grains (5,6). A further problem associated with the YBa$_2$Cu$_3$O$_{7-x}$ superconductors is incomplete oxygenation during processing or gradual loss of oxygen subsequently, especially at grain boundaries. Due to high solubility of oxygen in silver and presence of silver at grain bondaries, it is an efficient source of oxygen for the YBa$_2$Cu$_3$O$_{7-x}$ superconductor matrix.

Similarly, in an attempt to improve the critical current density and mechanical properties, several fabrication techniques have been studied to make bulk parts from pure YBa$_2$Cu$_3$O$_{7-x}$ or Ag-YBa$_2$Cu$_3$O$_{7-x}$ powders. High critical current density parts have been made by melt texturing (7) that results in oriented grained structures necessary for high critical current density. Other fabrication techniques such as cold pressing and sintering (8), tape casting (8), and powder-in-tube rolling (9), have used Ag and YBa$_2$Cu$_3$O$_{7-x}$ powder mix to improve the mechanical properties. Most of the studies done on fabrication employing Ag-YBa$_2$Cu$_3$O$_{7-x}$ systems have employed the powder metallurgy route of mixing elemental silver powder with YBa$_2$Cu$_3$O$_{7-x}$ powder in different proportions (5,6). This technique may result in rather non-homogeneous distribution of silver in YBa$_2$Cu$_3$O$_{7-x}$ matrix. In contrast to the powder metallurgy route of mixing powders, sol-gel co-precipitation provides a homogeneous distribution of various phases in composites.

In this study, we report on a technique for synthesizing fine, homogeneous Ag-$YBa_2Cu_3O_{7-x}$ composite powders by extending the citrate sol-gel technique proposed by Kakihana et al (10) to make single phase $YBa_2Cu_3O_{7-x}$ powders. We have also made an attempt to produce structurally sound dense parts of Ag-$YBa_2Cu_3O_{7-x}$ which have the potential of carrying high current densities. Porous preforms of $YBa_2Cu_3O_{7-x}$ were made, which were then infiltrated with silver to give dense parts. The porous preforms of near net shape were made by the rapid prototype technique - Selective Laser Sintering (SLS) (11,12).

SLS is a pressureless sintering process which usually involves a liquid phase (13). Partial liquid phase is formed and solidified as the laser beam is scanned across the powder bed in a directional fashion. Such directional formation and solidification of liquid phase can result in an oriented-grained structure. Since $YBa_2Cu_3O_{7-x}$ melts incongruently (14,15), it is possible to form partial liquid phase by careful control of the laser power density to induce interphase melting. Other laser processing parameters that affect the microstructure and hence the properties are : laser scan speed, scan spacing and the layer thickness. These laser processing parameters have been studied extensively for various ceramic, metals and polymer systems (12,13). By careful manipulation of these parameters and the powder characterstics such as particle size, desirable microstructure with optimum properties can be obtained.

EXPERIMENTAL PROCEDURE

SYNTHESIS OF $YBa_2Cu_3O_{7-x}$ And Ag-$YBa_2Cu_3O_{7-x}$ POWDERS

Metal nitrates, $Y(NO_3)_3$, $Ba(NO_3)_2$, $Cu(NO_3)_2$ and $AgNO_3$, were dissolved in water in required amounts. 1.9 g citric acid to 1 g of $Ba(NO_3)_2$ was dissolved in the nitrate solution. This was followed by addition of 10 ml of ethylene glycol per 1 mmol of Y. The ratios of citric acid to $Ba(NO_3)_2$ and ethyleneglycol to Y are same as that proposed by Kakihana et al (10) as the process is insensitive to pH. The amounts of various nitrates were varied to produce 10g batches of Ag-$YBa_2Cu_3O_{7-x}$ composite powders with compositions in the range 0 - 60 weight percent silver. All the solutions were heated on a hot plate at $100^{\circ}C$ - $150^{\circ}C$ to obtain a brown-black solid which was ground into powder and referred to as "precursor". The precursor was calcined at $900^{\circ}C$ in oxygen for 10-12 hours followed by furnace cooling. The calcined powder was ground and its structure and purity were assessed by x-ray diffraction. Following calcination, the powders were oxygen annealed at $600^{\circ}C$ for 6 hours.

SELECTIVE LASER SINTERING

The Selective Laser Sintering workstation system developed and described by Birmingham et al (13) was used to carry out the sintering. Pure $YBa_2Cu_3O_{7-x}$ and Ag-$YBa_2Cu_3O_{7-x}$ powders of compositions 20% and 30% by weight of silver, were used in this study. All SLS processing were carried out in air at room temperature. A 25 Watt CO_2 laser was used with a beam diameter of 700 μm. Three dimensional square parts of 8 mm side dimension were made layer by layer to final thicknesses ranging from 1 to 3 mm. Laser power density was varied from 500 W/cm^2 to 1300 W/cm^2. Laser scan speeds of 1 to 3 mm/second were employed. Scan spacing was kept constant at 100 μm for all runs. Layer thickness was varied from 250 μm to 150 μm. Initial layers were thicker (200-250 μm) to avoid displacement of the previously sintered layers by the roller action during the spreading of powder to lay fresh layers for sintering. As subsequent layers were sintered the layer thickness was gradually reduced to 150 μm. The final thickness of the sample was thus controlled by the layer thickness and the number of layers.

INFILTRATION

The porous parts obtained by SLS were infiltrated with silver to fill up the pores and provide a reinforcing ductile phase. Silver infiltration was accomplished by placing the samples in an alumina boat with sufficient silver powder (0.7-1.3 μm) atop the samples (16). The boat with the sample and infilterant was heated in a vertical tube furnace at 970°C in air for 10 to 30 minutes. The process was continuously monitored to allow melting of silver and its infiltration, by capillary effect, into the porous $YBa_2Cu_3O_{7-x}$ samples while avoiding any significant melting of the $YBa_2Cu_3O_{7-x}$ which would result in loss of shape.

CHARACTERIZATION

The SLS porous parts and the silver infiltrated dense parts were annealed at 930° C for 8 to 10 hours in flowing oxygen and slow cooled in flowing oxygen. Structural phases of the powders synthesized by sol-gel and of parts fabricated by SLS and infiltration were investigated at each stage of processing by X-ray diffraction. Critical transition temperatures were measured by a SQUID magnetometer. Samples were weighed before and after silver infitration to determine the volume fraction of porosity at each stage and to find the degree of silver infilteration. A Micromeritics Accupyc 1330 pycnometer was used to determine the degree of open versus closed porosity. The sample microstructures and the distribution of silver were studied by SEM.

RESULTS AND DISCUSSION

POWDER SYNTHESIS

Submicron (~100nm) size $YBa_2Cu_3O_{7-x}$ and $Ag-YBa_2Cu_3O_{7-x}$ powders were synthesized by the citrate sol-gel technique. X-ray diffraction spectra of $Ag-YBa_2Cu_3O_{7-x}$ composites with different weight percents silver are shown in Figure.1. The x-ray diffraction patterns show the orthorhombic $YBa_2Cu_3O_{7-x}$ structure for all samples. The x-ray peaks for silver are present as separate peaks suggesting that the silver is present as a separate crystalline phase in the $YBa_2Cu_3O_{7-x}$ matrix. However, in some samples of $Ag-YBa_2Cu_3O_{7-x}$, reflections from Y_2BaCuO_5 and/or $BaCuO_2$ are present. Presence of these impurity phases arise due to greater difficulty in complete and efficient removal of CO_2 evolved from the decomposition of citrate gel complexes during heat treatments. $YBa_2Cu_3O_{7-x}$ reacts strongly with CO_2 and the reaction products depend on the CO_2/O_2 ratio and the annealing temperature (17).

$YBa_2Cu_3O_{7-x}$ precursor derived from the gel decomposition requires calcination and oxygen annealing to obtain the superconducting orthorhombic structure. In this study, it was noticed that presence of silver had a significant effect on the degree of oxygen annealing required to obtain complete oxygenation of the $YBa_2Cu_3O_{7-x}$ structure. Batches of $Ag-YBa_2Cu_3O_{7-x}$ containing less than 30 weight percent silver required oxygen annealing following calcination to obtain superconducting orthorhombic structure. No such oxygen annealing was necessary for developing a completely oxygenated structure when batches of $Ag-YBa_2Cu_3O_{7-x}$ contained 30 weight percent or more silver. X-ray diffraction of powder samples from $Ag-YBa_2Cu_3O_{7-x}$ containing 20 and 30 weight percent silver without any oxygen annealing, Figure.2., indicate an incompletely oxygenated tetragonal structure for the lower silver content sample but completely oxygenated orthorhombic $YBa_2Cu_3O_{7-x}$ structure for the higher silver content sample. Table I shows the heat treatments required to obtain completely oxygenated orthorhombic $YBa_2Cu_3O_{7-x}$ structure in $Ag-YBa_2Cu_3O_{7-x}$ composites with different silver contents. Oxygenation of the $YBa_2Cu_3O_{7-x}$ structure occurs by diffusion during the heat treatment and subsequent cooling of the precursor. In this study it was seen that the process of diffusion is slow in bulk samples with low silver content while the diffusive process is enhanced by increasing the silver content. Also, it seems possible to decrease the time of calcination with increasing silver content.
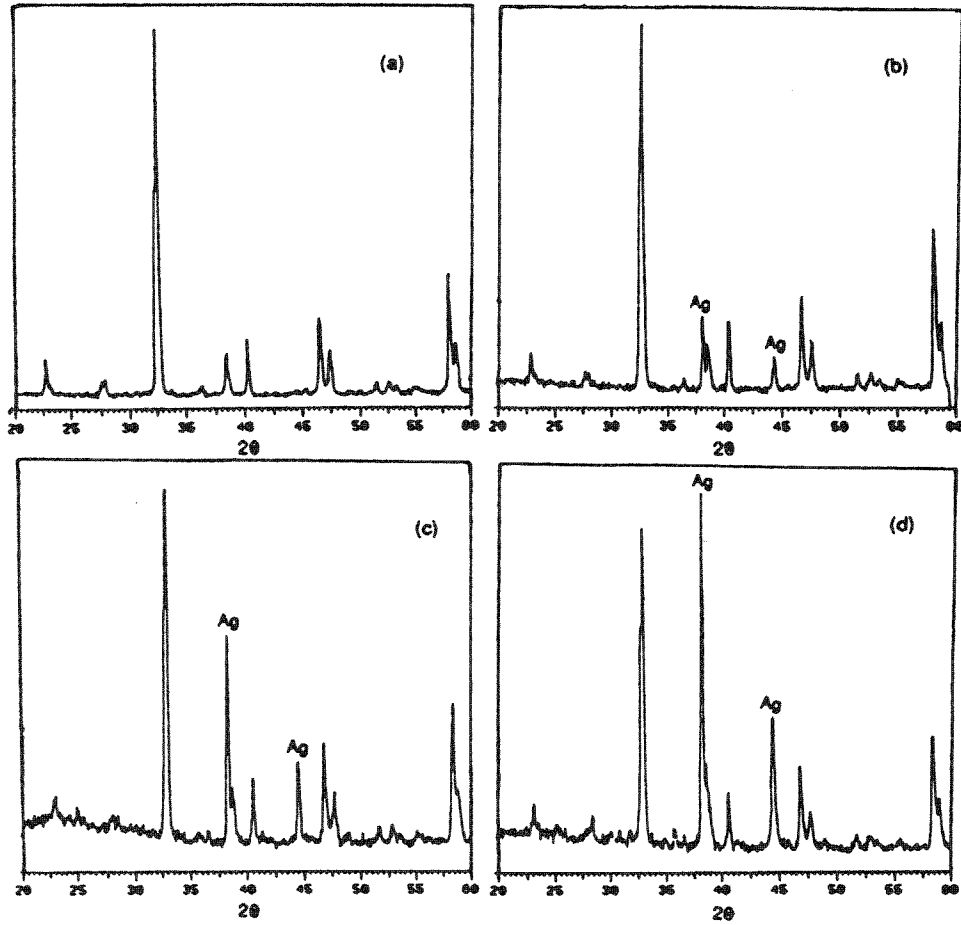
Fig.1. XRD Patterns of Ag-YBa$_2$Cu$_3$O$_{7-x}$ Composite Powders With Different Silver Contents Prepared by Sol-Gel Co-Precipitation (a) Pure YBa$_2$Cu$_3$O$_{7-x}$ (b) 20 Wt.% Ag - 80 Wt.% YBa$_2$Cu$_3$O$_{7-x}$ (c) 40 Wt.% Ag-60 Wt.% YBa$_2$Cu$_3$O$_{7-x}$ (d) 60 Wt.% Ag-40 Wt.% YBa$_2$Cu$_3$O$_{7-x}$
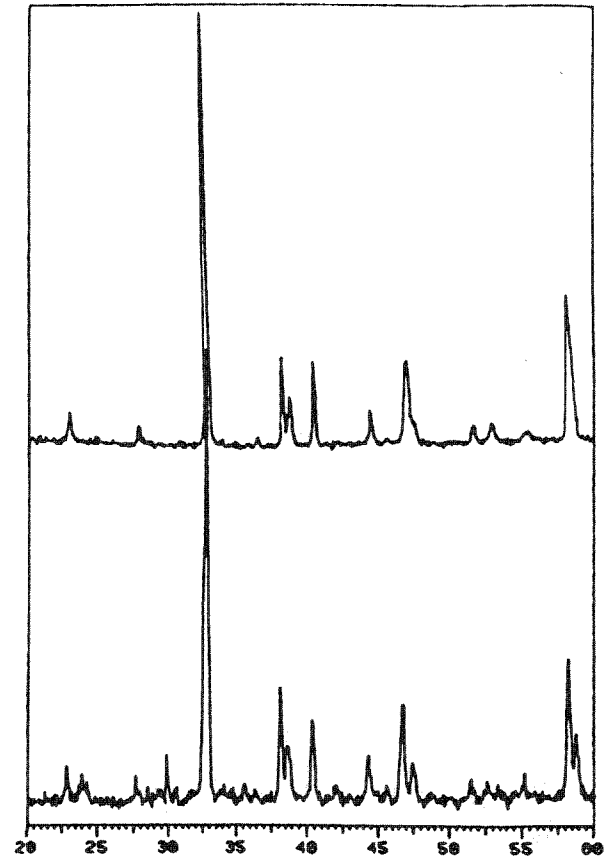
Fig.2. XRD Patterns of 20 Wt. % Ag - 80 Wt.% YBa$_2$Cu$_3$O$_{7-x}$ (top) and 30 Wt.% Ag-70 Wt.% YBa$_2$Cu$_3$O$_{7-x}$ (bottom), Both Having Undergone Calcination Prior to Oxygen Annealing.

The results of T_c measurements made on the $Ag-YBa_2Cu_3O_{7-x}$ powder composites with different silver contents are shown in Figure.3. As indicated in Table I, the onset T_c remains unaffected up to a silver content of 40 weight percent and decreases slightly above 40 weight percent. There is a slight broadening of the transition width with increasing silver content. Broadening of transition width is usually associated with presence of bulk second phase, silver in this study, especially at grain boundaries. However, in all cases, the materials exhibited zero T_c at temperatures well above liquid nitrogen temperature (77K).
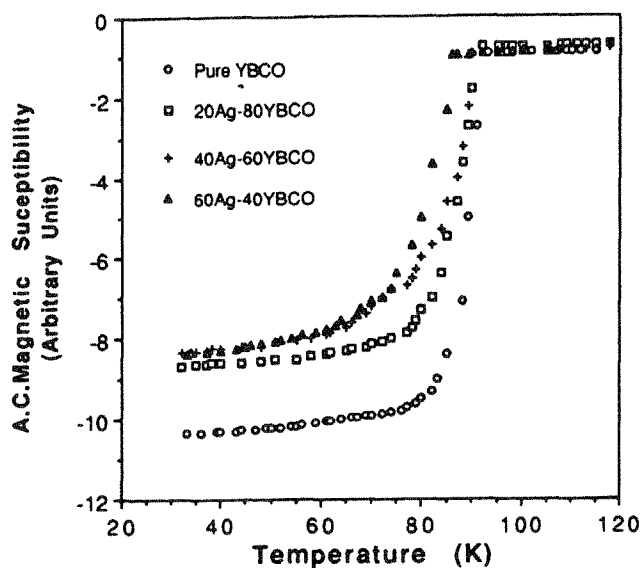

Fig.3. A.C. Magnetic Susceptibilty measurements as a function of temperature for $Ag-YBa_2Cu_3O_{7-x}$ composite powders.

Table I : Heat Treatments for Ag-$YBa_2Cu_3O_{7-x}$ Powders

Amount of Silver		Heat treatment	Onset T_c (K)
Wt %	Vol %		
0	0	Calcination And Oxygen Annealing	93
20	13.1	Calcination And Oxygen Annealing	92
30	20.62	Calcination Only	92
40	28.78	Calcination Only	91
50	37.74	Calcination Only	88
60	47.63	Calcination Only	86

SELECTIVE LASER SINTERING

Partial liquid phase, necessary for SLS, was created by providing sufficient laser power density to produce a temperature above the peritectic decomposition temperature of $YBa_2Cu_3O_{7-x}$, producing Y_2BaCuO_5 and a liquid phase, "L" according to the reaction (14,18) :

$$YBa_2Cu_3O_{7-x} \longrightarrow Y_2BaCuO_5 + "L"$$
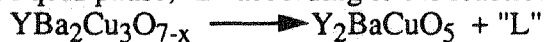
The amount of liquid phase, "L", formed depends on degree of peritectic superheating.

Single layer and multilayer tests of $Ag-YBa_2Cu_3O_{7-x}$,with 20 and 30 weight percent Ag, done at various scan speeds and laser power density did not produce a structurally sound part that could be handled successfully. However, similar tests with pure $YBa_2Cu_3O_{7-x}$ powder produced structurally sound parts at laser power densities above $500W/cm^2$. Lack of structural integrity in $Ag-YBa_2Cu_3O_{7-x}$ parts may be due to a decreased ratio of liquid to solid phase.

As shown in Figure 4(a), XRD patterns of selectively laser sintered parts did not exhibit significant crystallinity, irrespective of the laser processing parameters, but did indicate a breakdown of the $YBa_2Cu_3O_{7-x}$ structural phase into various phases, such as Y_2BaCuO_5, $BaCuO_{2-x}$ and $BaCu_2O_2$. The existance of metastable, noncrystalline phases is expected after SLS due to rapid melting and solidification of the ceramic $YBa_2Cu_3O_{7-x}$ in the process. However, following SLS, crystallinity and the superconducting phase, $YBa_2Cu_3O_{7-x}$ were restored in the SLS parts by oxygen annealing and slow, controlled cooling [Figures 4(b) and 4(c)]. Small

343

amounts of impurity phases of Y_2BaCuO_5, $BaCu_2O_2$ and $BaCuO_{2-x}$ were still found in the samples. As shown in Figures 4(b) and 4(c), samples processed at high laser power density (>1000 W/cm^2) had higher degree of non-superconducting phases present in them even after oxygen annealing. Higher laser power density raises the powder temperature enough to result in complete melting which leads to significant chemical segregation and complete breakdown of the $YBa_2Cu_3O_{7-x}$ structure. Such severe breakdown in structure makes it more difficult for the stoichiometric, orthorhombic structure to be regained completely during oxygen annealing at 930°C for 8 to 10 hours. Lower laser power density (<1000 W/cm^2) results in partial melting of the powders, according to the above mentioned peritectic reaction, resulting in partial breakdown of the $YBa_2Cu_3O_{7-x}$ structure and less chemical segregation. Therefore, nearly phase pure $YBa_2Cu_3O_{7-x}$ is easily regained by a simple oxygen annealing when the laser power density produces only a partial melting of the $YBa_2Cu_3O_{7-x}$ powders.
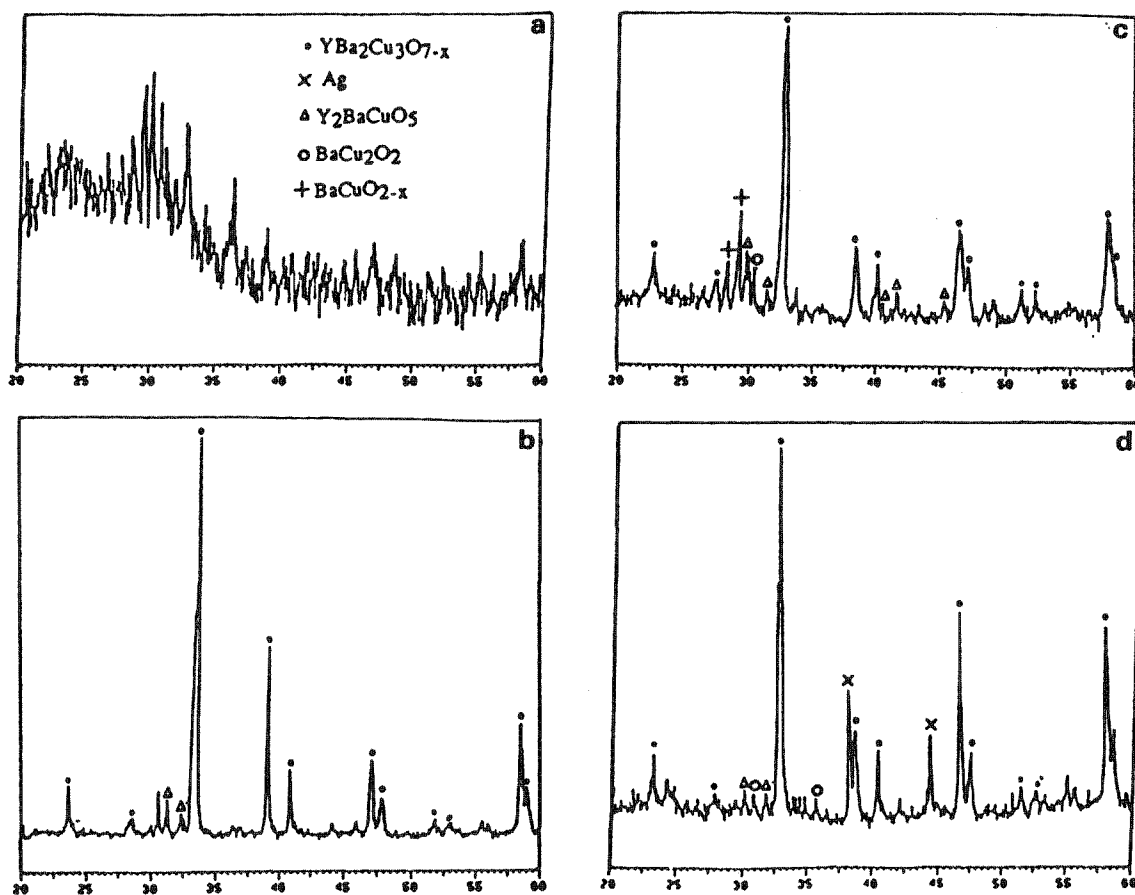

Figure 4. XRD Patterns of (a) SLS $YBa_2Cu_3O_{7-x}$, (b) SLS and O_2 Annealed $YBa_2Cu_3O_{7-x}$, Sample B, (c) SLS and O_2 Annnealed $YBa_2Cu_3O_{7-x}$, Sample D, and (d) SLS, Silver Infiltrated and O_2 Annealed $YBa_2Cu_3O_{7-x}$, Sample H.

Bulk density of various SLS metal and ceramic parts has been found to be affected by laser processing parameters. In this study, bulk density of the laser sintered $YBa_2Cu_3O_{7-x}$ parts varied from 55% to 75% of theoretical density as the laser power density increased from 500W/cm^2 to 1300W/cm^2 at a constant scan speed of 1mm/second (Figure 5). Bulk density also varied from 55% to 65% as the scan speed decreased from 2 to 1 mm/second at a constant power density of

$750W/cm^2$ (Figure 6). Reduced layer thickness was found to improve the bulk density significantly. However thick layers had to be used in the initial build-up of the structure to prevent displacement of the layers by the traversing roller. Density of the $YBa_2Cu_3O_{7-x}$ samples was also measured using the helium gas pycnometer. Using the theoretical density of $YBa_2Cu_3O_{7-x}$ and from the densties determined by the pycnometer, it was concluded that the porous, SLS parts had predominantly open, interconnected porosity with only 1% - 2% closed porosity.

Localized heating of the powder bed results in a temperature gradient along the scan line during SLS. If the temperature gradient is large, residual stresses appear in the sample which can lead to macrocracks and debonding of the layers. As shown in Figures 7(a) and 7(b), the surface and cross-section of a laser sintered part of $YBa_2Cu_3O_{7-x}$ show some macrocracks but no significant debonding of layers. High laser power density and low scan speeds, which tend to aggravate this problem, also produced no significant debonding of layers in $YBa_2Cu_3O_{7-x}$. Figures 7 also show high degree of open porosity on surface and cross-section which is most desirable for further densification by infiltration.

INFILTRATION

Oxygen annealing of SLS parts at 930°C for 8 to 10 hours restored the desired orthorhombic $YBa_2Cu_3O_{7-x}$ structural phase, but did not improve the bulk density of the samples significantly. Higher annealing temperatures (>940°C), for similar time periods, increased the bulk densities moderately but not significantly, but at a cost of partial or complete loss of shape. Partial liquid phase formation can occur in $YBa_2Cu_3O_{7-x}$ above 900°C by a eutectic reaction arising due to CuO and/or BaO enrichment in the stoichiometry. The temperature at which this eutectic occurs and the amount of liquid phase formed depends on the deviation from stoichiometry. Therefore, prior to oxygen annealing, densification of the porous SLS parts was achieved by infiltrating silver into the open interconnected pores. Infiltration was done at 970°C to insure melting of the silver (melting point at 960°C) for efficient infiltration. Higher infiltration temperatures lead to shape loss due to execessive melting of the $YBa_2Cu_3O_{7-x}$. For the same reason the infiltration process at 970°C was continously monitored and the process was stopped in 10 to 30 minutes when all the silver atop the $YBa_2Cu_3O_{7-x}$ samples had melted and infiltrated into the pores. Keeping the time periods for infiltration short prevented any loss of shape, even though the infiltration temperature (970°C) was above the eutectic tempearture. This is probably due to relatively small amount of liquid phase formed. However, such short time periods of infiltration did not result in restoration of the $YBa_2Cu_3O_{7-x}$ phase in the parts. Therefore, following SLS and silver infiltration, the samples were oxygen annealed at 930°C for 8 to 10 hours.

As shown in Figure 8, infiltration occurred throughout the cross-section of the sample with large, continuous pores being infiltrated completely by silver while infiltration into micropores was limited. This is probably due to the relatively high viscosity from the small superheating of the molten silver, thus hindering infiltration into micropores. The bulk density of the samples after silver infiltration was found to be 85% to 90%. The volume fraction of silver in the samples varied from 30% to 45% depending on the volume fraction of pores before infiltration and the extent of infiltration.

SQUID magnetometer T_c measurements for different samples are shown in Figure 9. T_c (onset) under zero field conditions for all the samples is approximately 88K to 90K. There is a slight broadening of the transition width for samples processed under aggressive laser conditions and also for the silver infiltrated parts. Transition width broadening is usually associated with the presence of bulk second phases. Parts processed under aggressive laser conditions have some impurity second phase, as evidenced from X-ray diffraction, which results in transition width broadening. Silver infiltrated parts have continuous networks of silver as a second phase causing
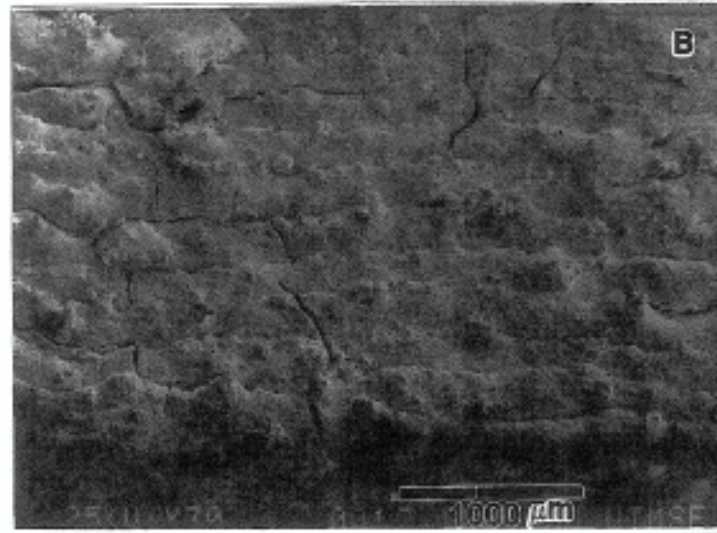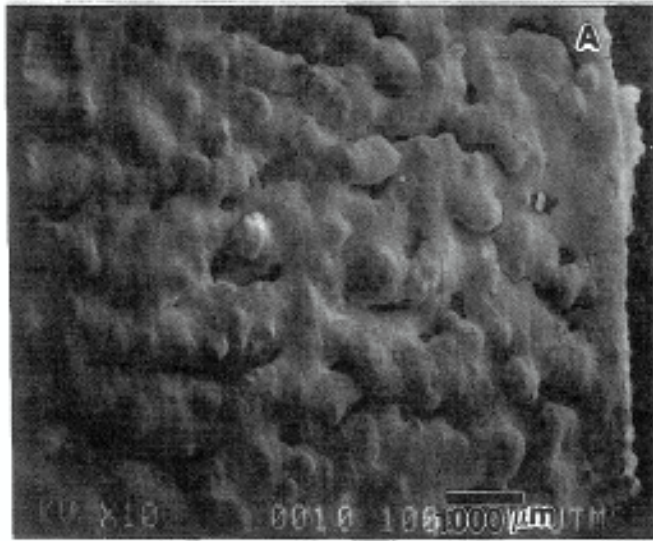
Figure 5. SEM Micrographs of a SLS YBa$_2$Cu$_3$O$_{7-x}$ Sample (A) Surface and, (B) Cross-section.
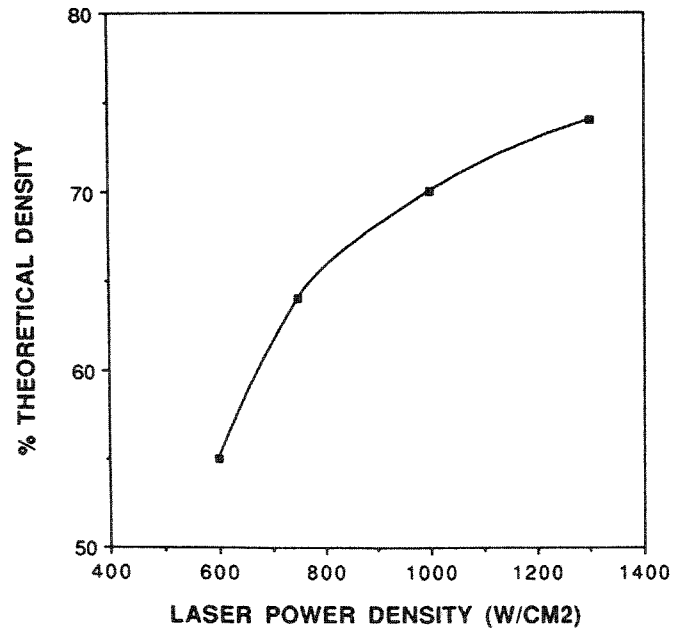
Figure 6. Bulk Density as a Function of Laser Power
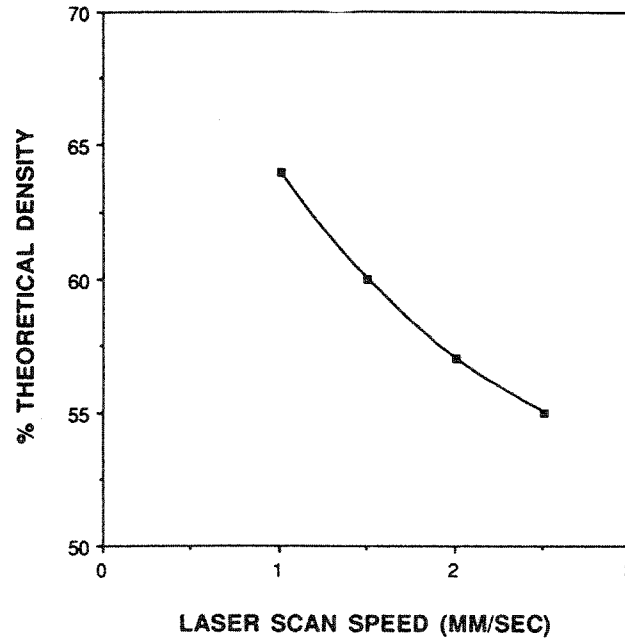

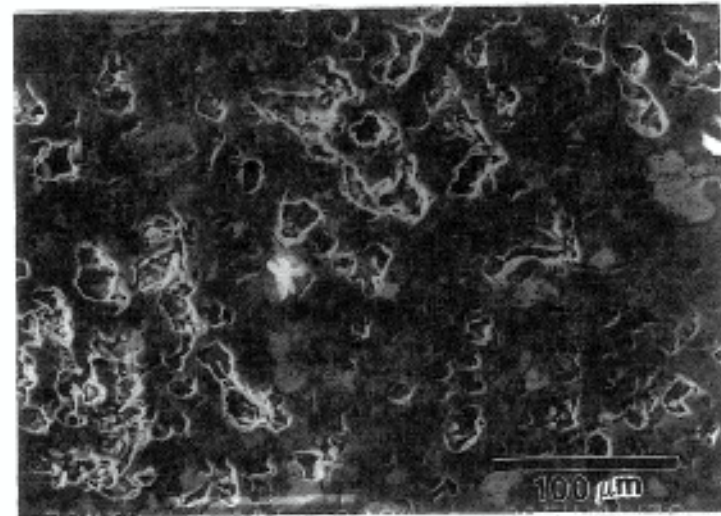Figure 7. Bulk Density as a Function of Laser Scan Speed.

Figure 8. SEM Micrographs of SLS and Silver Infiltrated $YBa_2Cu_3O_{7-x}$ Samples.
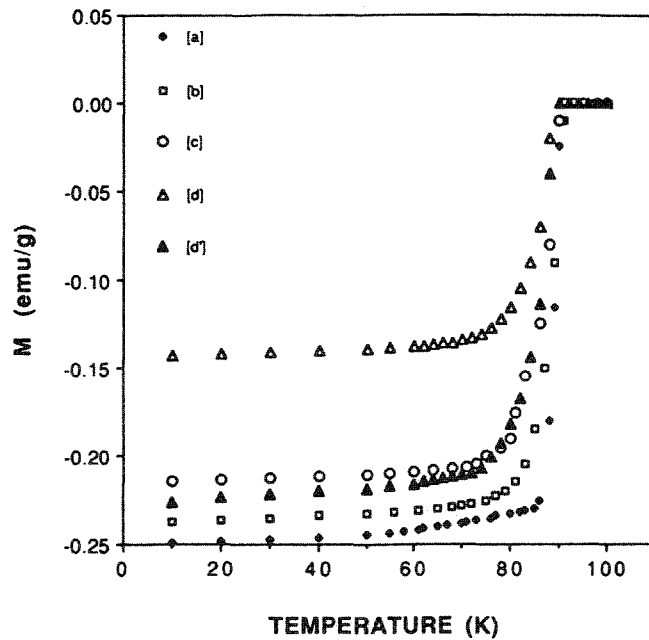
Figure 9. Field-Cooled (20 Gauss) Magnetization Data versus Temperature for [a] As Prepared $YBa_2Cu_3O_{7-x}$ Powders, [b] Low Laser Power SLS and O_2 Annealed $YBa_2Cu_3O_{7-x}$, Sample B, [c] High Laser Power SLS and O_2 Annealed $YBa_2Cu_3O_{7-x}$, Sample D, [d] Low Laser Power SLS, Silver Infiltrated and O_2 Annealed $YBa_2Cu_3O_{7-x}$, Sample H, and [d'] Data of curve (d) divided by (1- Ag weight fraction).

the broadening. However, in all cases, $T_c{}^{zero}$ occurs well above the liquid nitrogen temperature of 77K. Comparision of diamagnetic signals of samples processed by SLS and oxygen annealing (Figures 9b and 9c) with that of as prepared $YBa_2Cu_3O_{7-x}$ powders (Figure 9a) reveals that SLS followed by oxygen annealing does not result in any significant reduction in the fraction of superconducting phase. This is in good agreement with the XRD data which shows very small qunatities of non-superconducting phases after SLS and oxygen annealing. Similarly, comparision of Figures 9d' and 9a shows that silver infiltration in conjunction with SLS does not cause in any significant fraction of non-superconducting phases. This is also in good agreement with the XRD data and indicates that no chemical reaction occurs during silver infiltration to result in any non-superconducting phases, as also observed by other studies on Ag-$YBa_2Cu_3O_{7-x}$ composite studies (5,19).

TABLE   II. SLS Processing Parameters and Post-SLS
Processes Used.

Sample	Laser Power (W/cm^2)	Speed (mm/sec)	Ag Infiltration (970°C)	O$_2$ Anneal (930°C)
A	600	1.0	No	Yes
B	750	1.0	No	Yes
C	1000	1.0	No	Yes
D	1300	1.0	No	Yes
E	750	1.5	No	Yes
F	750	2.0	No	Yes
G	600	1.0	Yes	Yes
H	750	1.0	Yes	Yes
I	1000	1.0	Yes	Yes

CONCLUSIONS

Fine (~100 nm) powders of superconducting $YBa_2Cu_3O_{7-x}$ and Ag-$YBa_2Cu_3O_{7-x}$ were successfully synthesized by a simple sol-gel technique. Presence of silver in the $YBa_2Cu_3O_{7-x}$ aided in the oxygenation of the superconductor necessary during annealing. The fine powders were then successfully fabricated into bulk, porous shapes by selective laser sintering which were subsequently densified by silver infitration. The relationships between laser processing parameters and the resulting physical and superconducting properties can be summarised as follows :
(1) Bulk density of SLS $YBa_2Cu_3O_{7-x}$ parts improves with increased laser power density, reduced scan speed, and reduced layer thickness.
(2) Oxygen annealing restored nearly phase pure orthorhombic $YBa_2Cu_3O_{7-x}$ structure in parts processed under lower laser power density (<1000 W/cm^2).
(3) Silver was found to infiltrate successfully into large, continuous pores, improving the bulk density, while micropores were infiltrated partially.
(4) $T_c{}^{onset}$ for SLS parts and silver infiltrated parts were 88 K - 90K.
(5) Broad transition widths were observed for parts processed under high laser power and for those infiltrated with silver.

ACKNOWLEDGEMENTS

References

1. J.G.Bednorz, and K.A.Muller, "Possible High-T_c Superconductivity in the Ba-La-Cu-O System," Z. Phys. B: Condens. Matter 64, 189, (1986).

2. T.Venkatesan, X.D.Wu, B.Dutta, A.Inam, M.S.Hegde, D.M.Hwang, C.C.Chang, L.Nazar, and B.Wilkins, Appl. Phys. Lett., 54, 6, (1989).

3. R.C.Sherwood, S.Jin, T.H.Tiefel, R.B.Van Dover, R.A.Fastnacht, M.F.Yan and W.W.Rhodes, "Superconducting Properties of $YBa_2Cu_3O_{7-x}$ Doped with Various Metals and Oxides," Mat. Res. Soc. Symp. Proc. Vol. 99. 503-506 (1988).

4. M.F.Yan, W.W.Rhodes, and P.K.Gallagher, "Dopant Effects on the Superconductivity of $YBa_2Cu_3O_7$ Ceramics," J. Appl. Phys. 63(3) 821-828 (1988).

5. Y.Matsumotò, J.Hombo, Y.Yamaguchi, M.Nishida, and A.Chiba, "Origin of the Silver Doping Effects on Superconducting Oxide Ceramics," Appl. Phys. Lett., vol. 56 No. 16 1585-1587 (1990).

6. M.Itoh, H.Ishigaki, T.Ohyama, T.Minemoto, H.Nojiri, and M.Motokawa, "Influence of Silver on Critical Current of the Y-Ba-Cu-O Superconductor," J. Mater. Res. 6[11] 2272-2279 (1991).

7. S.Jin, T.H.Tiefel, R.C.Sherwood, R.B.Van Dover, M.E.Davis, G.W.Kammlott, and R.A.Fastnacht, "Melt Textured Growth of Polycrystalline $YBa_2Cu_3O_{7-x}$ with High Transport J_c at 77K," Phys. Rev. B, 37, 7850, (1988).

8. J.P.Singh, H.J.Leu, R.B.Poeppel, E.van Voorhees, G.T.Goudey, K.Winsley, and D.Shi, "Effect of Silver and Silver Oxide Additions on the Mechanical and Superconducting Properties of $YBa_2Cu_3O_{7-x}$ Superconductors," J. Appl. Phys., 66(7), 3154, (1989).

9. S.Sen, I.Chen, C.H.Chen, and D.M.Stefanescu, "Fabrication of Stable Superconductive Wires with $YBa_2Cu_3O_x/Ag_2O$ Composite Core," Appl. Phys. Lett., 54(8), 766, (1989).

10. M.Kakihana, L.Borjesson, S.Erikson, P.Svedlindh, and P.Norling, "Synthesis of Highly Pure $YBa_2Cu_3O_{7-x}$ Superconductors Using a Colloidal-Processing Technique," Physica C, 162, 931, (1989).

11. D.L.Bourell, H.L.Marcus, J.W.Barlow, and J.J.Beaman, "Selective Laser Sintering of Metals and Ceramics," Int. J. Powder. Met., 28(4), 369, (1992).

12. Proceedings of the Solid Freeform Fabrication Symposium, 1991. Edited by H.L.Marcus, J.J.Beaman, J.W.Barlow, D.L.Bourell, and R.H.Crawford, Aug. 12-14, 1991, The University of Texas at Austin, Austin, Texas.

13. Proceedings of the Solid Freeform Fabrication Symposium, 1992. Edited by H.L.Marcus, J.J.Beaman, J.W.Barlow, D.L.Bourell, and R.H.Crawford, Aug. 3-5, 1992, The University of Texas at Austin, Austin, Texas.

14. K.Oka, K.Nakane, M.Ito, M.Saito, and H.Unoki, "Phase-Equilibrium Diagram in the Ternary System Y_2O_3-BaO-CuO," Jpn. J. Appl. Phys., 27(6), L1065, (1988).

15. N.Nevriva, P.Holba, S.Durcok, D.Zemanova, E.Pollert, and A.Trisk, "On the Melt Equilibria in the Y-Ba-Cu-(O) System," Physica C, 157, 334, (1989)

16. R.M.German, "Phase Diagrams in Liquid Phase Sintering Treatments," J. Metals, 38(8), 26, (1986).

17. Y.Gao, K.L.Merkle, C.Zhang, U.Balachandran and R.B.Poeppel, "Decomposition of $YBa_2Cu_3O_7$ During Annealing in CO_2/O_2 Mixtures," J. Mater. Res. 5[7] 1363-1367 (1990).

18. N.Ozkan, B.A.Glowacki, E.A.Robinson, and P.A. Freeman, "Infrared Zone Melting Process for $YBa_2Cu_3O_{7-x}$ Wires," J. Mater. Res., 6(9), 1829, (1991).

19. B.Ropers, R.Canet, F.Carmona, and S.Flandrois, "Transport Properties and Percolating Behavior of YBaCuO/Ag Random Composites Above and Below T_c," Solid State Comm., 75(10), 791, (1990).